



	Experiment title: Stroboscopic X-ray magnetic circular dichroism study of dynamic component of the magnetic moment in strong	Experiment number: HC-2054
Beamline: ID12	Date of experiment: from: 18 Nov 2015 to: 23 Nov 2015	Date of report: <i>Received at ESRF:</i>
Shifts: 18	Local contact(s): Andrei Rogalev	

Names and affiliations of applicants (* indicates experimentalists):

CAMINALE Michael* - Laboratory CEA Grenoble - INAC SPINTEC, France

EBELS Ursula - Laboratory CEA Grenoble - INAC SPINTEC, France

BAILEY William* - Laboratory Columbia University Dept. of Applied Physics and Applied Math., USA

OLLEFS Katharina* - Faculty of Physics, University Duisburg-Essen, Germany

ROGALEV Andrei – ESRF, France

Report:

This beamtime had been granted 18 shifts, over the 36 asked, as a proof of principle study of the research activity presented in the proposal.

The main objectives of the present experiment were the following: (i) installation and alignment with the beam of the new experimental setup (Fig. 1A-B); (ii) measurement of magnetic X-ray reflectivity (MXR) at heavy metal L-edge in direct contact with the ferromagnetic material (Fig. 2); (iii) measurement of X-ray ferromagnetic resonance (XFMR) in longitudinal configuration, i.e. having the projection of the k-vector of the beam on the sample plane parallel to the applied bias field H_b (Fig. 3A-C).

The system under scrutiny was a sputtering deposited $\text{Py}(5 \text{ nm})/\text{Pt}(1 \text{ nm})_{\times 10}$ multilayer grown directly beneath the 300 nm thick Al line (silver u-shaped line on Si crystal in the center of Fig. 1B), fabricated by photolithography and lift-off procedures. The Si crystal was mounted on an Al support with two end launcher connectors for the transmission of the RF signal. The holder is clamped in the gap of the electromagnet as shown in Fig. 1A; the direction of the beam is depicted by the magenta dashed arrow.

The system was successfully aligned allowing the measurement of XMCD spectra in standard fluorescence detection (Fig. 4) and of MXR at different photon energies, i.e. before, after and at the Pt L3 absorption edge. In Fig. 2, reflectivity (black solid line, left axis) is plot as a function of the angle θ_2 , at the L3 edge. The intense broad peaks at 1.7 and 2.4 degree are ascribed to the magnetic multilayer, while the smaller oscillations to the thick Al film. By flipping a magnetic field of about 80 mT at each point, the magnetic contrast is measured. In Fig. 2 the magnetic contrast (red solid line, right axis) resulting from the average of right- and left-circular light polarizations is reported.

The measurement of XFMR is carried out monitoring the intensity of the reflected beam while sweeping the bias field H_b , at fixed photon energy (11.57 keV), incidence angle (0.66 degrees) and frequency of the resonance-driving RF field H_{RF} (5 GHz). A lockin-like detection was employed, that is the RF power was modulated at 67Hz between -20 and 37 dBm during the measurement. When the magnetization of Py is set in precession with a cone angle θ_p at the resonance field for that given driving frequency, the magnetization component lying on the plane will be reduced of a factor $1-\cos\theta_p$ inducing a change in the reflected beam. For 37 dBm (5 Watts) RF power a cone angle of about 3.7 degrees is estimated, resulting in an expected magnetic contrast $5E4$ times smaller of the one obtained for full magnetization reversal. Fig. 3A and B show XFMR measurement (blue noisy lines, right axis) averaged from 50 scans each (12hrs measuring time in total) for positive and negative sweeping field, respectively. As reference, the FMR traces (black solid lines, left axis) obtained measuring the outgoing RF power is also shown. The difference of the two traces for positive and negative bias field is reported in Fig. 3C, along with the estimated signal intensity (red dashed horizontal lines) for this configuration. We conclude that the noise is one order of magnitude larger of the expected signal in this longitudinal geometry. In the same resonance conditions, a 30 times larger signal is expected in transverse geometry, for which the maximum amplitude of the sinusoidal signal is proportional to $\sin\theta_p$.

Finally, in order to gain insights on the growth of the multilayer, propaedeutic additional measurements were also done on different magnetic stacks, to be employed as possible samples in the second part of the research study proposed. In particular the following heterostructures were measured: 1) Py(5 nm)/Pt(0.5 nm) \times_{20} , a thinner Pt layer with double number of repetition allowed to get a factor 2 larger XMCD signal due to a factor 2 larger surface to volume ratio, however less sharp reflectivity peaks were found; 2) Py(5 nm)/Cu(0.5, 1 nm)/Pt(1 nm) \times_{10} , by the insertion of 1 nm of a Cu interlayer no more static induced magnetic moment is detected on Pt by XMCD (Fig. 4), indicating that for 1 nm coverage a uniform film is formed in these growth conditions.



Fig. 1A

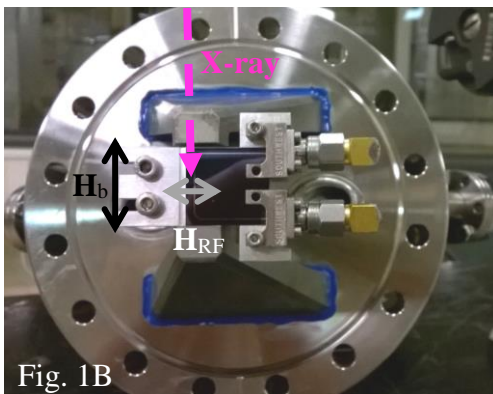


Fig. 1B

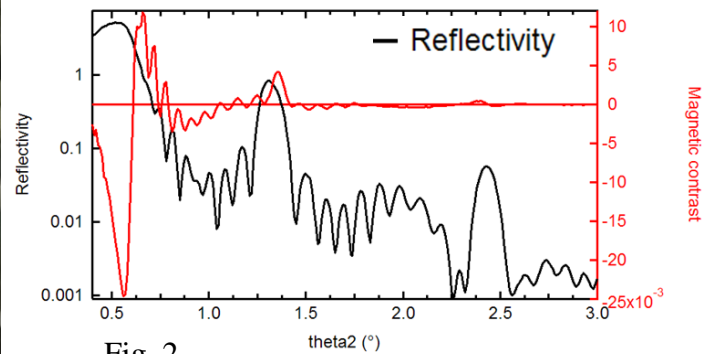


Fig. 2

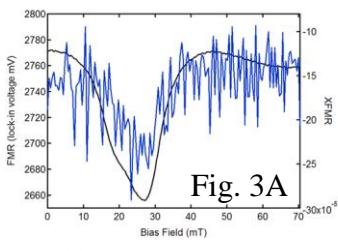


Fig. 3A

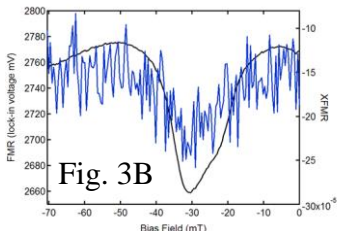


Fig. 3B

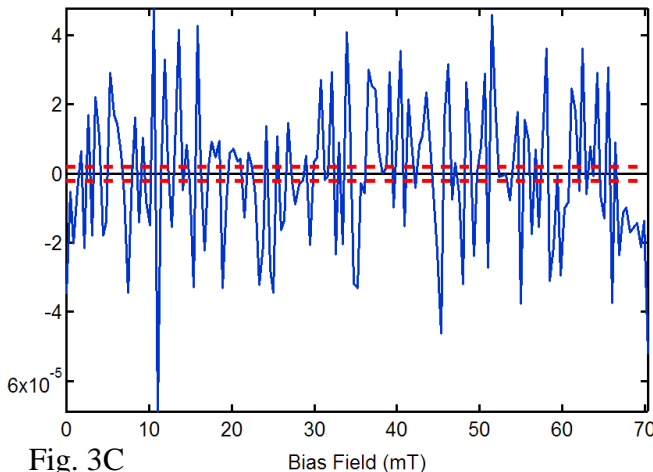


Fig. 3C

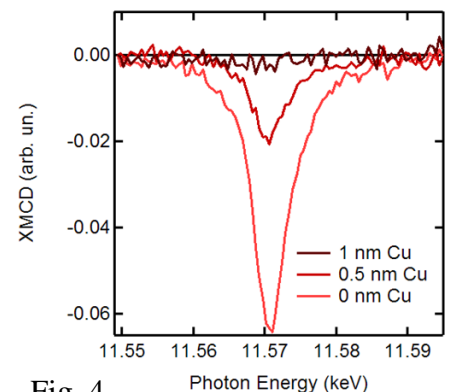


Fig. 4